

Pool-Select-Refine: Allocation-Aware Generative Dataset Distillation with Soft-Label-Guided Latent Refinement

Wenmin Li^a, Shunsuke Sakai^{a,*}, Zhongkai Zhao^b and Tatsuhito Hasegawa^{a,*}

^aGraduate School of Engineering, University of Fukui, 3-9-1 Bunkyo, Fukui, 910-8507, Fukui, Japan

^bCollege of Computer Science and Artificial Intelligence, Southwest Minzu University, No.168, Wenxing Section, Dajian Road, Konggang Development Zone, Shuangliu District, Sichuan, China

ARTICLE INFO

Keywords:

Dataset Distillation
Diffusion Models
Allocation Waste
Sample Selection
Latent Optimization
Soft Labels

ABSTRACT

Diffusion-based dataset distillation has recently emerged as a promising paradigm for condensing large-scale datasets into compact synthetic sets. By leveraging pretrained generative priors, these methods can produce realistic class-conditional samples more efficiently than traditional matching-based approaches. However, most existing diffusion-based methods still adopt a rigid “*Generate-and-Use*” strategy, where the generated samples are directly treated as the final distilled set under a fixed images-per-class budget. Such a design tightly couples candidate generation with final budget allocation, which may result in redundant waste of the limited budget or insufficiently informative samples. In this paper, we propose “*Pool-Select-Refine*”, a two-stage framework for allocation-aware generative dataset distillation. First, instead of directly using a fixed number of generated samples, we construct an over-complete candidate pool and select a compact subset under the target budget. Second, we refine the selected samples in latent space using soft-label supervision derived from the teacher model, improving semantic alignment while preserving the generative prior. This design explicitly decouples generation, selection, and refinement, enabling more effective use of the distillation budget. Experiments on large-scale and fine-grained image classification benchmarks show that the proposed framework delivers consistent gains over diffusion-based baselines. The results suggest that introducing a curation stage before refinement is a simple yet effective way to improve diffusion-based dataset distillation.

1. Introduction

The extraordinary achievements of deep learning are fundamentally driven by large-scale datasets. However, storing and training such massive datasets incurs prohibitive computational costs. To address these costs, Dataset Distillation (DD) [39] has emerged as a powerful paradigm. It aims to synthesize a small yet information-rich dataset on which models can be trained to achieve performance comparable to that of models trained on the full training dataset. Early approaches primarily focus on optimizing synthetic pixels through kernel-based [25, 46, 23] or matching-based strategies [1, 44, 43, 41, 11, 6, 38, 29, 33].

Recently, generative DD [42, 9, 2, 45, 35, 30, 3, 47, 24, 40, 37] has become a compelling alternative. Unlike matching-based methods that are constrained by high resolution requirements and memory usage, generative approaches leverage the rich priors of pre-trained models to efficiently synthesize diverse and informative samples. In this line of work, diffusion models (DMs) [15, 34] have emerged as a powerful generative framework that can produce realistic and diverse class-conditional samples with better training stability than traditional Generative Adversarial Networks (GANs) [8]. Some recent works [2, 9, 3] have started to exploit the capability of generative models, by introducing importance-aware objectives [9], influence-function-based guidance [3], and latent-space optimization [2].

*Corresponding author

✉ mf240815@e.u-fukui.ac.jp (W. Li)

ORCID(s): 0009-0004-6009-8668 (W. Li)

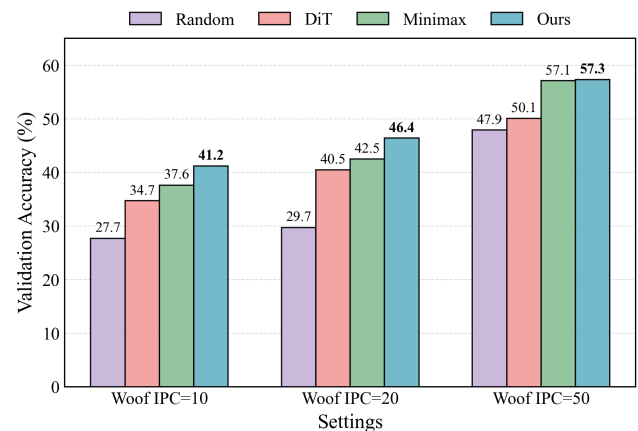


Figure 1: Performance comparison on ImageWoof under different IPC budgets. Our method consistently improves over the baselines under the same IPC budget, demonstrating the effectiveness of explicit curation and refinement for fine-grained dataset distillation.

However, the potential of diffusion-based distillation [9, 35, 30, 3, 47, 24, 40, 37] is not fully exploited by existing pipelines. Most current methods still follow a rigid “*Generate-and-Use*” paradigm: for each class, a fixed number of synthetic samples is generated to match the target IPC budget and then directly used as the final distilled set. Although this strategy is simple and efficient, it tightly couples candidate generation with final budget allocation. Since diffusion sampling is inherently stochastic, the generated samples may contain redundant modes, weakly informative instances, or semantically unstable candidates. As a result, a

Table 1

Mechanism-level comparison of representative DD methods. We focus on whether a method explicitly introduces a curation stage between candidate generation and final budget allocation, and whether the selected samples are further refined using teacher-derived semantic supervision. “✓” indicates explicit support, and “✗” indicates no support.

Method	Generative Prior	Explicit Curation Stage	Decouple Gen./Budget Allocation	Teacher Soft Targets Reused	Teacher-guided Latent Refinement
DM [43]	✗	✗	✗	✗	✗
TM [1]	✗	✗	✗	✗	✗
GLaD [2]	✓	✗	✗	✗	✗
Minimax [9]	✓	✗	✗	✗	✗
IGD [3]	✓	✗	✗	✗	✗
Ours (Pool-Select-Refine)	✓	✓	✓	✓	✓

non-trivial portion of the limited distillation budget can be wasted on samples with low information density.

From the perspective of DD, the key challenge is therefore not only to generate realistic samples, but also to decide which samples should occupy the limited IPC budget. This suggests a shift from one-shot data production to IPC-constrained curation: a generator can first produce an over-complete class-conditional candidate pool, and the final distilled set can then be selected from this pool according to sample usefulness. Such a decoupling allows diffusion generation to serve as a source of candidates rather than a direct replacement for the final distilled set, enabling better control over the semantic quality, diversity, and compactness of the selected samples.

Based on this idea, we propose “*Pool-Select-Refine*”, a two-stage framework for diffusion-based DD. To retain compact yet informative samples under the target IPC budget, in Stage I, we first construct an over-complete class-conditional candidate pool. Then, we perform IPC-constrained subset selection that jointly considers semantic reliability, feature-space diversity, and predictive uncertainty, reducing the risk of selecting redundant or semantically unstable candidates. While this curated subset contains compact yet informative samples, its semantic fidelity and quality are still not comparable to those of real samples. Therefore, in Stage II, we further refine the selected samples in latent space using teacher-derived soft-label supervision while preserving the pretrained generative prior [27]. This design excludes the additional fine-tuning stage for DMs, enabling efficient, fine-grained sample refinement.

Figure 2 illustrates the pipeline-level difference between conventional one-shot generate-and-use distillation and our proposed “*Pool-Select-Refine*” framework. The conventional pipeline directly trains the student on a fixed set of DiT-generated samples, so redundant or weakly informative samples may occupy scarce IPC slots. In contrast, our framework first builds an over-complete candidate pool, selects a compact subset according to reliability, diversity, and uncertainty, and then refines the selected samples before student training. This design makes the limited IPC budget more controllable and better aligned with the goal of dataset distillation.

Table 1 summarizes the mechanism-level differences between representative DD methods and our approach. Optimization-based methods such as DM [43] and TM [1] do not exploit generative priors, while recent generative

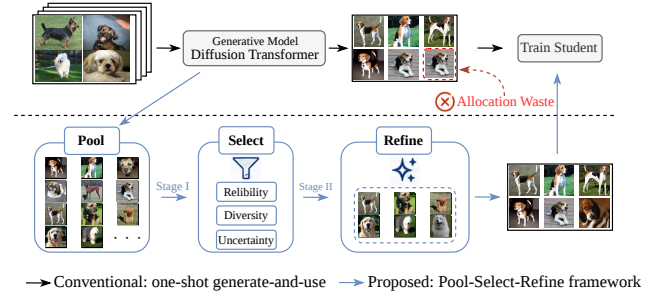


Figure 2: Pipeline comparison between conventional generate-and-use distillation and our Pool-Select-Refine framework. Instead of directly training the student on a fixed set of DiT-generated samples, our method first constructs an over-complete candidate pool, selects samples based on reliability, diversity, and uncertainty, and then refines the selected subset before student training.

methods such as GLaD [2], Minimax [9], and IGD [3] mainly improve the generation process itself. However, these methods still lack an explicit curation stage between candidate synthesis and final IPC allocation. In contrast, our “*Pool-Select-Refine*” framework explicitly decouples generation, selection, and refinement, and further reuses teacher soft targets for latent-space optimization. This distinction shifts diffusion-based distillation from simply producing realistic samples to making better use of each limited budget slot.

As shown in Figure 1, our method consistently improves over random real-data subsampling and diffusion-based generation baselines on the fine-grained ImageWoof benchmark across different IPC budgets. Notably, the gains are more pronounced under low-budget settings, where effective sample allocation is particularly important. Extensive experiments further demonstrate that the proposed framework consistently improves the corresponding diffusion-based baselines on ImageNet subsets and fine-grained benchmarks, while remaining competitive on CIFAR-scale datasets. These results support our central claim that explicit curation and refinement can make better use of the limited IPC budget in diffusion-based DD.

The key contributions of this work are as follows:

1. We point out that existing diffusion-based DD methods suffer from **allocation waste** due to the rigid “*Generate-and-Use*” paradigm, where limited IPC

budgets are directly spent on synthetic samples without an explicit curation stage.

2. We propose a two-stage “*Pool-Select-Refine*” framework to address this issue, which first performs IPC-constrained pool selection and then conducts soft-label-guided latent refinement on the selected samples.
3. Our framework is generic and easy to integrate with diffusion-based distillation pipelines, delivering consistent improvements on ImageNet subsets and fine-grained settings while remaining competitive on CIFAR benchmarks.

2. Preliminary

2.1. Generative DD

Unlike optimization-based approaches that directly update synthetic pixel values to match training gradients [41, 38, 29, 33] or optimization trajectories [1, 11, 6, 4], generative DD seeks to encode dataset knowledge [14] into the parameters or latent spaces of a generative model. This paradigm synthesizes informative samples on-the-fly or generates a static distilled set for student training.

GAN-based Approaches. Early generative distillation methods primarily utilized GANs [8]. For instance, IT-GAN [42] and other GAN-based priors [2, 45] invert the distillation process to optimize latent codes or generator parameters, aiming to synthesize images that minimize the student’s training loss. Although these methods reduce storage overhead compared to storing raw pixels, they often inherit inherent limitations of GANs, such as training instability and mode collapse, which hinder the diversity of distilled data [42, 2].

Diffusion-based Approaches. In recent years, DMs [26, 28, 15, 34, 18, 16] have surpassed GANs in generative distillation due to their superior training stability and broader pattern coverage. Their core principle involves constructing synthetic data distributions that match the statistical characteristics of teacher models through iterative denoising processes. Methods such as D4M [35] and Minimax Diffusion [9] model the distillation process as a minimax game or a gradient-matching problem within the diffusion dynamics, optimizing generation conditions to effectively reduce the validation loss of the student model. Meanwhile, recent research such as IGD [3] focuses on manipulating the sampling process or latent trajectories to maximize information gain.

Despite their success, existing diffusion-based pipelines typically follow a rigid “*Generate-and-Use*” paradigm, where a fixed number of samples equal to the target IPC are directly generated and used for student training. While simple and efficient, this design tightly couples candidate generation with final budget allocation, leaving little room for post-generation curation. Because diffusion sampling is inherently stochastic, the resulting fixed number of samples may contain redundant modes or weakly informative samples, causing a non-trivial portion of the limited distillation

budget to be wasted. This observation motivates the need for an explicit curation stage between generation and final usage, so that the limited IPC budget can be allocated to more useful synthetic samples.

2.2. Teacher-Derived Signals for IPC-constrained curation

Under a fixed IPC budget, the key challenge is not only to synthesize realistic candidates, but also to allocate a limited number of slots to the most useful ones. Once an over-complete class-conditional candidate pool \mathcal{P}_c is available, candidate curation becomes a crucial step for improving IPC budget utilization. The goal is to select a compact subset \mathcal{S}_c with $|\mathcal{S}_c| = K$ that preserves semantic reliability while maintaining sufficient coverage of the candidate pool. Teacher-derived confidence and feature-space coverage provide two useful signals for this purpose, although neither of them is sufficient on its own.

High-confidence Filtering. Since candidates in \mathcal{P}_c are generated conditioned on class c , a natural measure of reliability is the teacher probability assigned to the target class [13]:

$$s_{rel}(x) = q_T^c(c | x), \quad (1)$$

where $q_T^c(c | x)$ denotes the temperature-scaled softmax probability predicted by the teacher T for class c . This criterion prioritizes samples that are semantically consistent with the intended class. However, when used alone, it may over-concentrate the limited budget on easy and highly prototypical modes, thereby reducing the overall coverage of the selected subset.

Cluster-based Selection. To improve subset coverage, geometric strategies such as K-Center or K-Means select samples that spread the feature space [31]. Let $e_T(x)$ be the feature embedding extracted from the teacher T . The goal is to find a subset \mathcal{S}_c^* that minimizes the encoding error:

$$\mathcal{S}_c^* = \operatorname{argmin}_{\mathcal{S} \subset \mathcal{P}_c, |\mathcal{S}|=K} \sum_{x \in \mathcal{P}_c, x' \in \mathcal{S}} \min \|e_T(x) - e_T(x')\|_2^2. \quad (2)$$

Such strategies help prevent the selected subset from collapsing to a few dominant modes and therefore improve feature-space coverage. However, when used alone, geometric coverage may allocate budget to ambiguous or weakly reliable candidates. This suggests that effective curation should balance semantic reliability and coverage rather than relying on either signal in isolation.

2.3. Latent Diffusion Models

Latent Diffusion Models (LDMs) [28] perform the generative process in the compressed latent space of a pre-trained Variational Autoencoder (VAE). Let $\mathcal{E}(\cdot)$ and $\mathcal{D}(\cdot)$ be the VAE encoder and decoder, respectively. An image x is first mapped to a latent code $z_0 = \mathcal{E}(x)$. The diffusion process adds Gaussian noise to z_0 over T timesteps, producing a sequence z_1, \dots, z_T . For a generation, a denoising network $\epsilon_\theta(z_t, t, y)$ is trained to predict the added noise ϵ conditioned on the time step t and class label y . The standard training

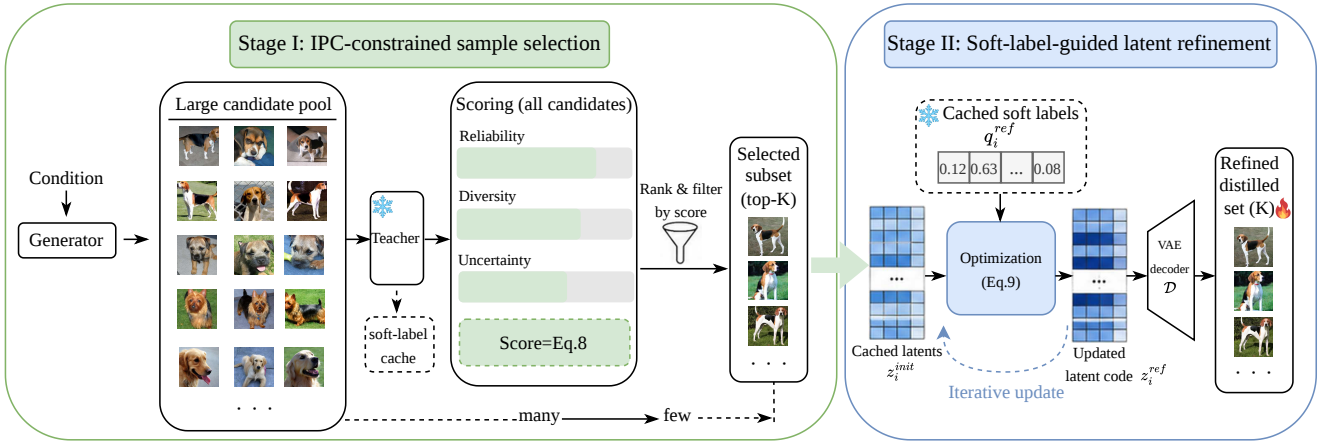


Figure 3: Detailed workflow of the proposed Pool-Select-Refine framework. Stage I constructs an over-complete candidate pool, evaluates all candidates using teacher-derived reliability, diversity, and uncertainty, and selects a compact subset under the target IPC budget. The teacher soft labels and generation latents of the selected samples are cached. Stage II directly optimizes the cached latent codes under soft-label guidance and decodes the refined latents into the final distilled set for student training.

objective is to minimize the simple mean-squared error:

$$\mathcal{L}_{\text{LDM}} = \mathbb{E}_{x, \epsilon \sim \mathcal{N}(\mathbf{0}, \mathbf{I}), t} [\|\epsilon - \epsilon_{\theta}(z_t, t, y)\|_2^2], \quad (3)$$

where $z_t = \sqrt{\bar{\alpha}_t} z_0 + \sqrt{1 - \bar{\alpha}_t} \epsilon_t$ and $\bar{\alpha}_t$ controls the noise schedule. In our framework, this denoising objective is later reused during latent refinement as an on-manifold regularizer, encouraging the optimized latent codes to remain consistent with the pretrained diffusion prior.

3. Proposed Method

As illustrated in Figure 3, the proposed “*Pool-Select-Refine*” framework consists of two consecutive stages: IPC-constrained pool selection and soft-label-guided latent refinement. Given a target IPC budget, Stage I first generates an over-complete class-conditional candidate pool and selects a compact subset according to teacher-derived reliability, feature-space diversity, and predictive uncertainty. For the selected samples, we cache both their teacher soft labels and generation latents. Stage II then directly refines the cached latent codes using the cached teacher soft labels while freezing the weights of the pretrained generative prior. The final refined samples, together with their teacher soft targets, are used to train the student model.

3.1. Motivation and Problem Formulation

We consider DD with C classes and a fixed budget of K IPC. Let T denote a fixed teacher model and S a student model to be trained on the distilled set. The goal is to construct a compact distilled dataset:

$$\mathcal{D}^* = \bigcup_{c=1}^C \{(x_{c,k}, q_{c,k}^{\text{ref}})\}_{k=1}^K, \quad (4)$$

where $x_{c,k}$ is the final distilled sample for class c , and $q_{c,k}^{\text{ref}}$ denotes its associated teacher soft target. Unlike rigid “*Generate-and-Use*” pipelines that directly treat exactly K

generated samples as the final distilled dataset, we start from an over-complete class-conditional candidate pool. Specifically, for each class c , a pretrained generator G produces:

$$\mathcal{P}_c = \{(z_j^{\text{init}}, x_j^{\text{init}})\}_{j=1}^M, \quad M > K, \quad (5)$$

where z_j^{init} is the latent code and $x_j^{\text{init}} = \text{Dec}(z_j^{\text{init}})$ is the decoded candidate image. This reformulation turns diffusion-based distillation from direct generation into a budget allocation problem: *given a limited budget K , how can we assign the final slots to the most useful candidates in \mathcal{P}_c ?*

Figure 4 provides empirical motivation for this formulation. Compared with directly using a fixed number of generated samples, selecting K samples from an over-complete pool consistently improves student performance. This indicates that budget waste is not only a generation-quality issue, but also a budget-allocation issue. Therefore, Stage I focuses on selecting more useful seeds from the candidate pool. Since each selected seed retains its cached latent z_i^{init} and teacher soft target q_i^{ref} , Stage II can further refine the selected samples directly in latent space without re-encoding the images.

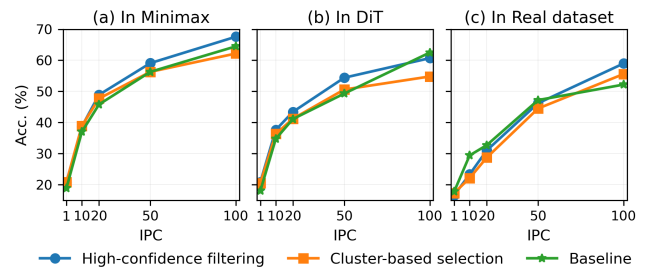


Figure 4: Accuracy comparison of different sample selection strategies across various IPC settings.

3.2. IPC-constrained pool selection

The goal of Stage I is not merely to discard low-quality candidates, but to allocate the limited IPC budget to samples that are most useful for student training. To evaluate the usefulness of generated candidates, we draw inspiration from three related lines of work: confidence-based reliability estimation [13], temperature-scaled probability calibration [10], core-set selection for diversity-aware data selection [31], and uncertainty sampling in active learning [32]. Specifically, teacher confidence provides a natural signal for measuring whether a generated candidate is semantically consistent with the target class, while core-set selection suggests that selected samples should be complementary and cover different regions of the feature space. In addition, predictive entropy reflects the ambiguity of the teacher prediction; unlike standard active learning that often queries uncertain real samples for annotation, we penalize excessive uncertainty because ambiguous synthetic candidates may waste scarce IPC slots. Inspired by these observations, we propose three complementary selection metrics: semantic reliability, feature-space diversity, and predictive uncertainty.

Reliability (s_{rel}). Following the reliability signal defined as Equation (1), we evaluate whether a candidate is semantically consistent with its target class. Candidates whose teacher-predicted label disagrees with c are discarded:

$$\arg \max_k q_T^c(k | x) \neq c.$$

This avoids allocating budget to samples with semantic drift.

Uncertainty (s_{ent}). Reliability alone is insufficient, because some candidates may still exhibit ambiguous or unstable semantic predictions. To suppress such samples, we introduce an uncertainty penalty based on the normalized predictive entropy:

$$s_{ent}(x) = -\frac{1}{\log C} \sum_{k=1}^C q_T^c(k | x) \log q_T^c(k | x), \quad (6)$$

where τ is the temperature scaling parameter. Higher entropy indicates greater semantic ambiguity; therefore, this term is subtracted in the final score to discourage uncertain candidates from consuming scarce budget.

Diversity (s_{div}). Under a fixed IPC budget, selecting only high-confidence samples tends to over-concentrate the subset on a few easy and prototypical modes. To improve coverage, we encourage diversity in the teacher feature space. Let $e_T(x)$ denote the teacher embedding of x . We define the diversity of a candidate as its distance to the nearest sample in the currently selected subset:

$$s_{div}(x) = \min_{x' \in S_c} \|e_T(x) - e_T(x')\|_2^2. \quad (7)$$

Maximizing this term helps prevent budget collapse onto a narrow region of the candidate pool and encourages the selected subset to cover complementary modes.

Composite Score and Greedy Selection. We combine the above three criteria into a unified allocation-aware scoring

rule. To reduce scale mismatch, each term can be optionally min-max normalized over the pool \mathcal{P}_c . The final score for a candidate x is defined as:

$$s(x) = \alpha s_{rel}(x) - \beta s_{ent}(x) + \gamma s_{div}(x), \quad (8)$$

where $\alpha, \beta, \gamma > 0$ are hyperparameters controlling the trade-off among semantic correctness, ambiguity suppression, and subset coverage. The weights α, β, γ are set according to the ablation study (Section 4.3.1).

Given an over-complete class-conditional candidate pool \mathcal{P}_c , the goal of Stage I is to allocate the fixed class budget K to a compact subset $S_c \subset \mathcal{P}_c$ with $|S_c| = K$ that is most useful for downstream student training. We evaluate each candidate $x \in \mathcal{P}_c$ using a composite score that integrates these three criteria.

We adopt a greedy selection strategy to construct S_c . The subset is initialized with the candidate having the highest reliability score. Then, at each step, we add the candidate that maximizes $s(x)$ and update the diversity term s_{div} with respect to the current subset. This process continues until K samples are selected.

3.3. Soft-Label-Guided Latent Refinement

Stage I improves IPC budget utilization by selecting better seeds from the over-complete candidate pool. However, the selected subset still consists of the best available candidates in the current pool, rather than the final optimum for student training. If these seeds are used directly, the limited IPC budget may still be occupied by samples whose semantic alignment and local sample quality remain suboptimal. Therefore, Stage II further refines each selected seed in latent space, so that every allocated budget slot becomes more useful before the final student training stage.

For each selected seed $(z_i^{\text{init}}, x_i^{\text{init}}) \in S_c$, we directly use the cached generation latent z_i^{init} as the optimization variable. Unlike methods that re-encode selected images, our refinement starts from the latent code already used to generate the selected candidate. We optimize only this latent variable while keeping the pretrained generator and VAE decoder frozen. After optimization, the refined latent is denoted as z_i^{ref} , and the corresponding refined image is obtained by $x_i^{\text{ref}} = \text{Dec}(z_i^{\text{ref}})$. This design preserves the generative prior and avoids modifying the backbone generator during distillation. We optimize each selected latent using

$$\mathcal{L}_{\text{lat}}(z) = \mathcal{L}_{\text{LDM}}(z) + w_i \mathcal{L}_{\text{KL}}(z), \quad (9)$$

where \mathcal{L}_{LDM} is the denoising objective reused from Section 2.3 as an on-manifold regularizer, and \mathcal{L}_{KL} aligns the refined sample with the cached teacher soft target associated with the selected seed. The effect of soft-label supervision is analyzed in Section 4.3.2.

Sample-adaptive weighting. Let $p_i = q_T^c(c | x_i^{\text{init}})$ denote the cached target-class confidence of the selected seed. We use

$$w_i = \lambda \cdot (w_{\min} + (1 - p_i)(w_{\max} - w_{\min})), \quad (10)$$

so that less confident seeds receive stronger semantic alignment, while highly reliable seeds are refined more conservatively. For efficiency, we adopt a late-stage schedule by disabling \mathcal{L}_{KL} during the first $L - R$ refinement iterations and enabling it only in the final R steps. This allows the latent to first adapt to the diffusion prior and then receive stronger semantic correction near the end of refinement.

After refinement, each refined image $x_i^{\text{ref}} = \text{Dec}(z_i^{\text{ref}})$ is paired with its cached teacher soft target q_i^{ref} and added to the final distilled set. The student training protocol on these refined pairs is summarized in Section 3.4.

3.4. Algorithmic Flow and Student Training

Algorithm 1 summarizes the full “*Pool-Select-Refine*” pipeline. For each class, we first construct an over-complete candidate pool, allocate the fixed IPC budget through Stage I selection, and then refine the selected seeds in latent space via Stage II before forming the final distilled set. After Stage II, the final distilled set is represented as pairs $(x_i^{\text{ref}}, q_i^{\text{ref}})$, where $x_i^{\text{ref}} = \text{Dec}(z_i^{\text{ref}})$ is the refined distilled image and q_i^{ref} is the cached teacher soft target inherited from the selected

Algorithm 1 Pool-Select-Refine

Ensure: Distilled set D^*
Require: Teacher T , generator G (decoder Dec), student S ; classes C ; IPC K ; pool size M ; temperature τ ; weights (α, β, γ) ; refine params $(\lambda, w_{\min}, w_{\max}, \eta, L, R)$.

- 1: $D^* \leftarrow \emptyset$
- 2: **for** $c = 1$ to C **do**
- 3: Sample $\{z_i^{\text{init}}\}_{i=1}^M \sim p(z | c)$
- 4: Decode candidates $x_i^{\text{init}} \leftarrow \text{Dec}(z_i^{\text{init}})$
- 5: Query teacher soft labels $q_i \leftarrow q_T^r(\cdot | x_i^{\text{init}})$
- 6: Extract teacher embeddings $e_i \leftarrow e_T(x_i^{\text{init}})$
- 7: Keep only samples predicted as class c by T
- 8: Initialize selected set $S_c \leftarrow \emptyset$
- 9: **for** $t = 1$ to K **do**
- 10: Pick next index $i^* \in \mathcal{I}_c \setminus S_c$
- 11: Update selection score with Equation (8)
- 12: $S_c \leftarrow S_c \cup \{i^*\}$
- 13: **end for**
- 14: **for** each $i \in S_c$ **do**
- 15: Cache teacher target $q_i^{\text{ref}} \leftarrow q_i$
- 16: Initialize latent $z \leftarrow z_i^{\text{init}}$
- 17: Update adaptive weight w_i with Equation (10)
- 18: **for** $\ell = 1$ to L **do**
- 19: Update objective with Equation (9)
- 20: Apply late-stage KL only if $\ell > L - R$
- 21: $z \leftarrow z - \eta \nabla_z \mathcal{L}_{\text{lat}}$
- 22: **end for**
- 23: Set $z_i^{\text{ref}} \leftarrow z$
- 24: Add refined pair $(\text{Dec}(z_i^{\text{ref}}), q_i^{\text{ref}})$ into D^*
- 25: **end for**
- 26: **end for**
- 27: Train student S on D^* with Equation (11)
- 28: **return** D^*

seed. The student is then trained on D^* using temperature-scaled knowledge distillation:

$$\mathcal{L}_{\text{KD}} = \frac{\tau^2}{|D^*|} \sum_{(x^{\text{ref}}, q^{\text{ref}}) \in D^*} \text{KL}\left(q^{\text{ref}} \parallel q_S^r(\cdot | x^{\text{ref}})\right). \quad (11)$$

Unless otherwise stated, this KD objective is used as the default student training protocol throughout the paper. For completeness, we also compare against hard-label supervision in the Section 4.3.3.

4. Experiments

4.1. Setting

We evaluate our method on multiple distillation settings with varying dataset scales and architectures. Table 2 reports results on ImageWoof using three student architectures: ConvNet-6, ResNet-AP-10, and ResNet-18, following prior work [7, 12]. We test five IPC levels, $K \in \{1, 10, 20, 50, 100\}$, covering both extremely low-data and relatively relaxed regimes. The teacher is a pretrained ConvNeXt-B [22], and the evaluation metric is top-1 accuracy reported as mean \pm standard deviation over three runs. We use the released generative/distillation pipelines of DiT and Minimax to synthesize class-conditional candidate pools; “Minimax” in the tables refers to the corresponding baseline distillation pipeline. Unless otherwise stated, we set the sampling steps = 50, candidate pool size to $M \geq 2K$, use temperature $\tau = 1.5$, optimize each selected latent for $L = 100$ iterations with learning rate $\eta = 0.01$, and set $\lambda = 0.5$, $w_{\min} = 0.1$, $w_{\max} = 2.0$, and $R = 4$ for Stage II refinement.

For Stage I selection, we use an IPC-dependent preset for (α, β, γ) : (3.0, 1.0, 0.5) for $K \leq 10$, (1.0, 1.0, 1.0) for $K = 20$, and (0.5, 1.0, 3.0) for $K \geq 50$. Unless otherwise stated, all student models are trained from scratch on the refined distilled pairs (x, q^{ref}) using the temperature-scaled KD objective in Section 3.4.

4.2. Results on ImageNet Subsets

Table 2 reports the main results on ImageWoof across five IPC settings and three student architectures. Our method consistently improves over its corresponding diffusion-based generators under the same generative prior. In particular, Minimax-Ours achieves consistent gains over Minimax across all IPC levels and evaluation models, while DiT-Ours also stably improves upon DiT and remains competitive with strong prior baselines. These results support our central claim: under a fixed IPC budget, explicitly decoupling candidate generation from IPC-constrained curation and subsequent refinement leads to more effective use of the distilled budget than directly adopting a rigid “*Generate-and-Use*” pipeline.

Table 3 further evaluates the proposed framework on two fine-grained ImageNet subsets, ImageNette [5, 17] and ImageIDC [5, 41], where classes exhibit higher intra-class similarity and are therefore more challenging for compact

Table 2

Quantitative results. Comparison of classification accuracy (%) under different IPC settings on ImageWoof subsets. Mnimax-Ours consistently outperforms baselines under all IPC levels, DiT-Ours consistently improves over DiT and is competitive with prior baselines (with some settings where DM remains stronger). Notably, under extremely low IPC (e.g., IPC=1), our distilled sets maintain strong generalization, substantially improves over baselines under extreme low IPC. N/A means the referenced method does not report results for the corresponding IPC/model configuration, so a direct comparison is unavailable.

IPC (Ratio)	Test Model	Random	DM [43]	IDC-1 [19]	GLaD [2]	RDED [36]	DiT	Minimax	DiT-Ours	Minimax-Ours	Full
1 (0.08%)	ConvNet-6	14.2 ± 0.9	21.1 ± 0.5	N/A	N/A	18.5 ± 0.9	12.7 ± 0.6	15.2 ± 0.6	18.9 ± 0.4	21.5 ± 0.9	86.4 ± 0.2
	ResNetAP-10	17.8 ± 2.4	N/A	N/A	N/A	N/A	18.0 ± 1.3	18.9 ± 2.4	22.8 ± 1.2	23.1 ± 1.5	87.5 ± 0.5
	ResNet-18	13.5 ± 0.4	N/A	N/A	N/A	20.8 ± 1.2	15.3 ± 0.7	14.6 ± 0.6	20.7 ± 0.5	21.9 ± 0.9	89.3 ± 1.2
10 (0.4%)	ConvNet-6	24.3 ± 1.1	26.9 ± 1.2	33.3 ± 1.1	33.8 ± 0.9	40.6 ± 2.0	34.2 ± 1.1	37.0 ± 1.0	40.6 ± 0.8	40.8 ± 1.3	86.4 ± 0.2
	ResNetAP-10	29.4 ± 0.8	30.3 ± 1.2	39.1 ± 0.5	32.9 ± 0.9	N/A	34.7 ± 0.5	39.2 ± 1.3	42.0 ± 0.7	40.8 ± 0.4	87.5 ± 0.5
	ResNet-18	27.7 ± 0.9	33.4 ± 0.7	37.3 ± 0.2	31.7 ± 0.8	38.5 ± 2.1	34.7 ± 0.4	37.6 ± 0.9	41.2 ± 0.3	39.3 ± 0.9	89.3 ± 1.2
20 (1.6%)	ConvNet-6	29.1 ± 0.7	29.9 ± 1.0	35.5 ± 0.8	N/A	N/A	36.1 ± 0.8	37.6 ± 0.2	45.6 ± 1.1	48.4 ± 0.8	86.4 ± 0.2
	ResNetAP-10	32.7 ± 0.4	35.2 ± 0.6	43.3 ± 0.3	N/A	N/A	41.1 ± 0.8	45.8 ± 0.5	48.2 ± 1.7	50.4 ± 0.7	87.5 ± 0.5
	ResNet-18	29.7 ± 0.5	29.8 ± 1.7	38.6 ± 0.2	N/A	N/A	40.5 ± 0.5	42.5 ± 0.6	46.4 ± 0.6	47.6 ± 1.3	89.3 ± 1.2
50 (3.8%)	ConvNet-6	41.3 ± 0.6	44.4 ± 1.0	43.9 ± 1.2	N/A	61.5 ± 0.3	46.5 ± 0.8	53.9 ± 0.6	56.6 ± 0.7	62.9 ± 1.0	86.4 ± 0.2
	ResNetAP-10	47.2 ± 1.3	47.1 ± 1.1	48.3 ± 1.0	N/A	N/A	49.3 ± 0.2	56.3 ± 1.0	58.8 ± 0.6	63.8 ± 1.6	87.5 ± 0.5
	ResNet-18	47.9 ± 1.8	46.2 ± 0.6	48.3 ± 0.8	N/A	N/A	50.1 ± 0.5	57.1 ± 0.6	57.3 ± 1.8	62.7 ± 0.4	89.3 ± 1.2
100 (7.7%)	ConvNet-6	52.2 ± 0.4	55.0 ± 1.3	53.2 ± 0.9	N/A	N/A	53.4 ± 0.3	61.1 ± 0.7	60.9 ± 0.4	68.7 ± 1.2	86.4 ± 0.2
	ResNetAP-10	59.4 ± 1.0	56.4 ± 0.8	56.1 ± 0.9	N/A	N/A	58.3 ± 0.8	64.5 ± 0.2	63.6 ± 0.6	72.6 ± 1.1	87.5 ± 0.5
	ResNet-18	61.5 ± 1.3	60.2 ± 1.0	58.3 ± 1.2	N/A	N/A	58.9 ± 1.3	65.7 ± 0.4	62.4 ± 1.2	69.8 ± 1.4	89.3 ± 1.2

Table 3

Comparison of test accuracy (%) on ImageNette/IDC under different IPC settings. Minimax-Ours consistently achieves the best performance; DiT-Ours improves upon DiT and is competitive across settings.

	IPC	Random	DiT	Minimax	DiT-Ours	Minimax-Ours
Nette	10	54.2 ± 1.6	59.1 ± 0.7	62.0 ± 0.2	60.2 ± 1.0	63.1 ± 1.9
	20	63.5 ± 0.5	64.8 ± 1.2	66.8 ± 0.4	66.7 ± 0.8	68.3 ± 0.9
	50	76.1 ± 1.1	73.3 ± 0.9	76.6 ± 0.2	78.7 ± 1.1	81.1 ± 1.7
IDC	10	48.1 ± 0.8	54.1 ± 0.4	53.1 ± 0.2	56.6 ± 0.5	54.8 ± 1.5
	20	52.5 ± 0.9	58.9 ± 0.2	59.0 ± 0.4	62.7 ± 0.6	65.3 ± 1.1
	50	68.1 ± 0.7	64.3 ± 0.6	69.6 ± 0.2	67.8 ± 1.6	70.8 ± 1.4

distillation. The same trend remains clear. Minimax-Ours consistently achieves the strongest performance, and DiT-Ours generally improves upon DiT while remaining competitive across settings. These results indicate that the proposed two-stage design is not limited to coarse-grained scenarios: even in fine-grained regimes, explicitly introducing a curation stage before latent refinement helps allocate limited budget to more useful synthetic samples.

4.3. Ablation

4.3.1. Complementarity of selection signals

To investigate the impact of each scoring component in our selection strategy, we conduct an ablation study in which only one of the three terms—reliability, uncertainty, or diversity—is activated at a time. As shown in Figure 5(a), the reliability term (Rel) achieves the best performance in low-budget regimes (IPC ≤ 10), while the diversity term (Div) gradually outperforms the others as IPC increases. The uncertainty term (Unc), when used alone, is less effective,

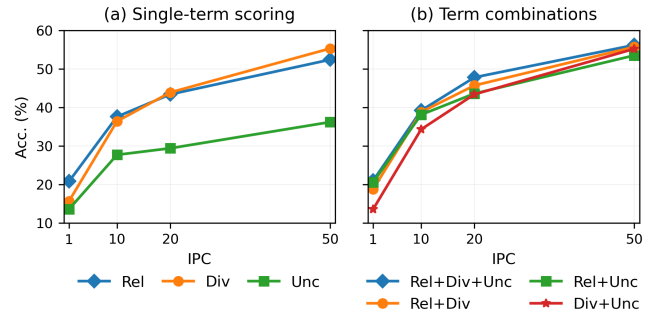


Figure 5: Ablation of selection signals under a DiT generative prior. (a) Single-term scoring using reliability, diversity, or uncertainty. (b) Pairwise and full combinations. Pairwise scoring consistently improves over single-term variants, and using all three signals achieves the best or tied-best accuracy across IPC settings, indicating complementary roles in subset curation.

especially in small-IPC settings.

Importantly, Figure 5(b) demonstrates synergy: any pairwise combination consistently outperforms the corresponding single-term variants, and combining all three signals yields the best (or tied-best) performance across IPC settings. This supports our design choice in Section 3.2 to score candidates jointly by reliability, diversity, and uncertainty rather than relying on a single heuristic.

Based on this, we use a simple preset schedule (chosen once from Figure 5 and fixed for all datasets/backbones). For low-data regimes ($K \leq 10$), we set $(\alpha, \beta, \gamma) = (3.0, 1.0, 0.5)$ to prioritize semantic correctness. For large budgets ($K \geq 50$), we set $(\alpha, \beta, \gamma) = (0.5, 1.0, 3.0)$ to emphasize coverage. For intermediate budgets (e.g., $K = 20$), we use the balanced

setting $(\alpha, \beta, \gamma) = (1.0, 1.0, 1.0)$. All weights are shared across classes within the same generator.

4.3.2. Effectiveness of Soft-Label KL in Latent Optimization

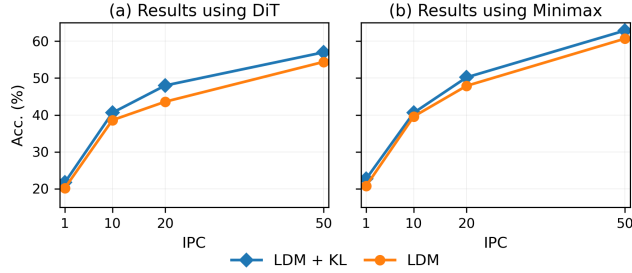


Figure 6: Effect of soft-label guidance in latent-space optimization. We compare the final classification accuracy between latent optimization with (LDM + KL) and without KL. Results on both DiT-based (a) and Minimax-based (b) pipelines demonstrate consistent performance improvement from soft-label supervision in the latent space.

We further validate the role of the soft-label KL divergence term in the latent optimization stage. As shown in Figure 6, adding the KL loss on top of the LDM [28] consistency significantly improves performance across all IPC settings. The improvement is particularly noticeable in medium and high IPC ranges, suggesting that aligning latent samples with teacher-predicted soft targets helps guide the optimization toward more class-discriminative and semantically aligned representations. Based on these observations, we include the KL term in the refinement objective for all experiments, using the late-stage schedule described in Section 3.3.

4.3.3. Soft Labels v.s. Hard Labels in Student Training

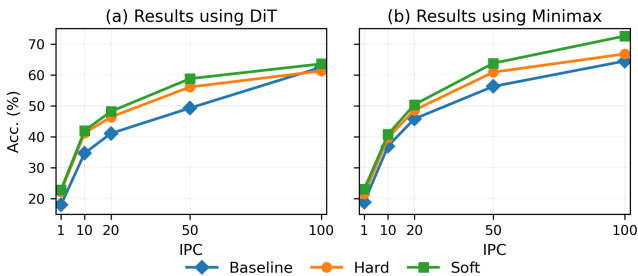


Figure 7: Comparison of soft-label and hard-label supervision when training models on distilled datasets. We report classification accuracy using three label settings—baseline (from original synthetic data), hard labels and soft labels. Across both DiT (a) and Minimax (b) pipelines, soft-label training consistently yields superior accuracy, especially under low IPC conditions.

Finally, we compare the effect of using soft labels versus hard labels when training the student network on the selected synthetic samples. Figure 7 summarizes the accuracy under both settings using DiT and Minimax [9] generators, respectively. Across all IPC levels, soft-label supervision yields

equal or better accuracy than hard labels, with consistent gains in the medium to high IPC range. This supports the intuition that soft targets provide richer inter-class relations and prevent over-confident predictions during low-data training. We therefore adopt soft labels by default in the student distillation phase.

4.4. Analysis of Hyperparameters

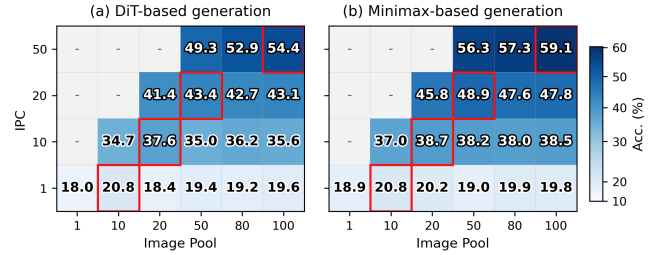


Figure 8: Heatmaps of classification accuracy over combinations of per-class image pool sizes and IPC. Each cell shows the classification accuracy when K samples from a pool of size M per class. Red boxes indicate the best configuration for each target IPC.

A critical hyperparameter is the size of the candidate pool M . Figure 8 presents the accuracy heatmaps for varying pool sizes versus target IPC (K). We observe a clear linear scaling law: the optimal pool size is approximately $2 \times K$ (twice the target IPC).

Too small ($M \approx K$). The selection space is overly constrained, degenerating into direct generation.

Too large ($M \gg 2K$). Performance tends toward saturation or shows slight decline, likely due to the inclusion of outliers in the candidate pool. This finding provides practical guidance for future research: merely doubling the budget yields selection advantages while keeping computational overhead within manageable limits.

4.5. Visualization

To intuitively assess the quality of the distilled dataset, we visualize the synthesized samples in Figure 9. We compare the images generated by our proposed method (applied to both DiT and Minimax backbones) against the original images and standard Minimax [9] baseline.

Visual Fidelity and Reliability. As observed in the “Golden Retriever” class, the baseline (Minimax) occasionally generates samples with blurred backgrounds or insufficiently defined facial features. In contrast, samples generated by Minimax-Ours exhibit greater visual *typicality*—capturing key semantic features with exceptional sharpness, such as fur texture and nasal structure. This qualitative leap validates our reliability-based selection strategy, which effectively filters low-quality or noisy modes within the candidate pool.

Semantic Alignment and Diversity. Within the *church* class, real images exhibit significant variations in lighting and architectural structures. Our approach (DiT-Ours) successfully synthesizes diverse architectural styles—such as varying spire shapes and viewpoints—while maintaining structural consistency. Unlike baseline models prone

Pool-Select-Refine for Generative Distillation

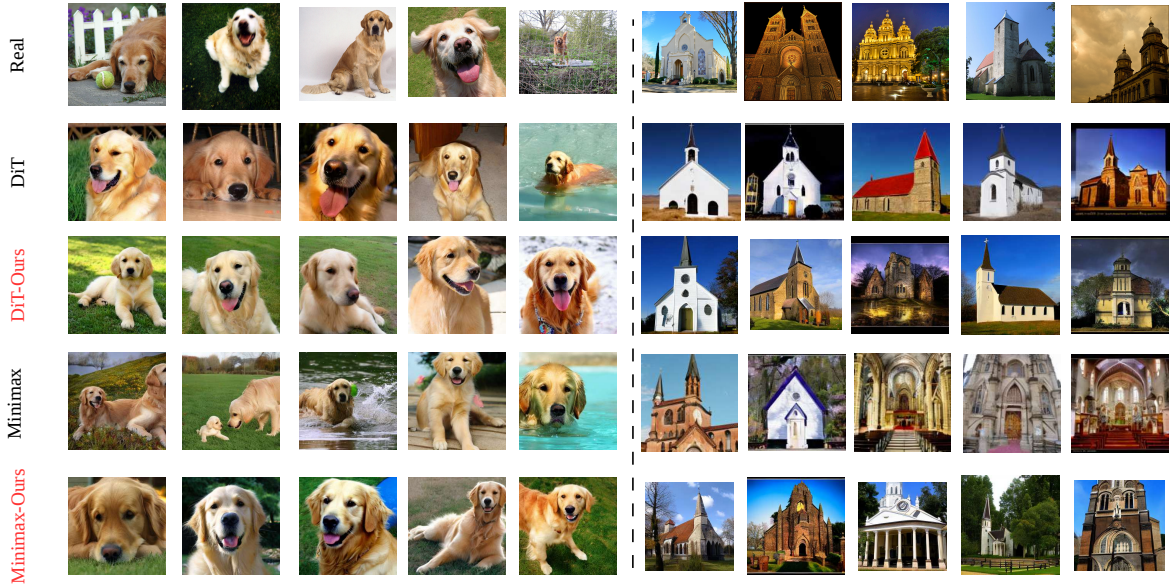


Figure 9: Qualitative visualization of distilled samples. We compare images from the Real dataset (Top row) against synthetic samples generated by standard baselines (DiT, Minimax) and our proposed method (DiT-Ours, Minimax-Ours). Columns exhibit samples from the *Golden Retriever* and *Church* classes. Compared to the direct generation baselines, which occasionally yield ambiguous backgrounds or artifacts, our method synthesizes images with higher semantic fidelity and clearer structural details (e.g., distinct facial features of dogs and architectural geometry of churches), demonstrating the efficacy of our diversity-aware selection and latent refinement.

to geometric distortions, our samples preserve sharp edges and accurate perspective effects. This structural integrity stems primarily from our soft-label-guided latent optimization technique—which forces the latent encoder to closely align with the teacher’s precise semantic understanding, correcting latent artifacts before final decoding.

These visual results confirm that our performance gains (Tables 2 and 3) are not merely numerical artifacts but stem from a tangible improvement in the semantic density and visual quality of the synthetic data.

5. Conclusion

This paper identified **allocation waste** as a key limitation of diffusion-based DD under the rigid “*Generate-and-Use*” paradigm. To address it, we proposed “*Pool-Select-Refine*”, a two-stage framework that first allocates the fixed IPC budget through explicit pool-based curation and then further refines the selected samples in latent space using teacher soft-label supervision. Experiments on ImageNet subsets, fine-grained benchmarks, and CIFAR demonstrate consistent gains over the corresponding diffusion-based baselines on large-scale and fine-grained settings, while remaining competitive on CIFAR. These findings indicate that introducing an explicit curation stage before refinement is an effective way to improve IPC budget utilization in diffusion-based DD.

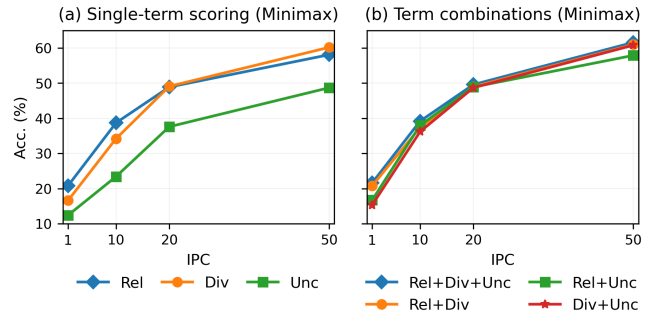


Figure 10: Complementarity of selection signals under a Minimax generative prior. (a) Single-term scoring using reliability, diversity or uncertainty. (b) Term combinations. Pairwise combinations generally outperform single-term variants, and combining all three signals yields the best or tied-best performance across IPC settings, indicating complementary roles in subset curation.

A. My Appendix

A.1. Complementarity of selection signals in Minimax

To verify that the observed complementarity is not specific to a particular generator, we repeat the scoring ablation using Minimax Diffusion as the generative prior, following the same protocol as in Section 4.3.1. Figure 10(a) shows that single-term scoring is insufficient: reliability tends to be more effective in low-IPC regimes, while diversity becomes increasingly important as IPC grows; using uncertainty alone remains less competitive. More importantly,

Table 4

Performance comparison on CIFAR-10, CIFAR-100, and Tiny-ImageNet under IPC = 1, 10, and 50. Our method (DiT-Ours) achieves strong performance across datasets, outperforming DM/DC on CIFAR-100 and Tiny-ImageNet across IPC settings, and showing clear gains on CIFAR-10 at higher IPC (e.g., IPC=50). N/A means the referenced method does not report results for the corresponding IPC/model configuration, so a direct comparison is unavailable.

IPC	CIFAR-10			CIFAR-100			Tiny-ImageNet		
	1	10	50	1	10	50	1	10	50
DM	26.0±0.8	48.9±0.6	63.0±0.4	11.4±0.3	29.7±0.3	43.6±0.4	3.9±0.2	12.9±0.4	24.1±0.3
DC	28.3±0.5	44.9±0.5	53.9±0.5	12.8±0.3	25.2±0.3	N/A	N/A	N/A	N/A
<u>DiT-Ours</u>	22.3±0.8	45.7±0.6	66.8±1.1	16.4±0.9	46.2±0.7	56.8±0.5	15.6±0.2	35.9±0.6	42.8±1.2

Table 5

Cross-architecture performance.

Model	ConvNet-6	ResNetAP-10	ResNet-18
Minimax-IGD	63.0	71.5	72.1
<u>Minimax-Ours</u>	68.7	72.6	69.8

Table 6

Comparison of integration results between our method and existing distillation approaches. N/A means the referenced method does not report results for the corresponding IPC/model configuration, so a direct comparison is unavailable.

IPC	10	50	100
DiT + IGD	41.0	62.7	69.7
<u>DiT + IGD + Ours</u>	42.3	65.6	76.4
MTT + GLaD	17.1	N/A	N/A
<u>MTT + GLaD + Ours</u>	22.6	30.8	55.1

Figure 10(b) indicates clear synergy—pairwise combinations generally improve over single-term variants, and the full combination (Rel+Div+Unc) achieves the best (or near-best) accuracy across IPC settings. These results mirror the DiT-based observations in Section 4.3.1, supporting the conclusion that our composite scoring captures complementary cues and transfers across diffusion-based generators.

A.2. Distill other datasets

To assess the generality of our method beyond ImageNet subsets, we further evaluate it on CIFAR-10, CIFAR-100 [20], and Tiny-ImageNet [21]. As shown in Table 4, our method outperforms DM [43] and DC [44] on CIFAR-100 and Tiny-ImageNet across IPC settings. On CIFAR-10, our method becomes advantageous at higher IPC (e.g., IPC=50), while remaining competitive at IPC=1/10.

A.3. IGD vs. Ours

We compare our method with Minimax-IGD [3], a prior approach that distills image gradients into synthetic data to improved generalization. As shown in Table 5, our method achieves consistent performance gains on ConvNet-6 and ResNetAP-10, outperforming IGD by 5.7% and 1.1%, respectively. On ResNet-18, although IGD slightly surpasses

our method by 2.3%, we note that our approach is model-agnostic and does not rely on architecture-specific gradient matching. These results support the robustness of our paradigm, especially under lightweight or shallow model settings, where soft label supervision and latent optimization contribute more significantly.

A.4. Combined with other methods

To verify the compatibility and generality of our strategy, we integrate our selection and optimization approach with two strong existing distillation frameworks: DiT+IGD [3] and MTT+GLaD [2]. As shown in Table 6, our method consistently improves classification accuracy across different IPC levels and distillation backbones. For instance, on DiT+IGD, the gain is particularly significant at IPC=100 (+6.7%), and for MTT+GLaD, our strategy boosts the previously underperforming IPC=10 case from 17.1% to 22.6%. These results confirm that our strategy is not only plug-and-play but also broadly effective, suggesting the potential for future unification across generative and trajectory-based distillation paradigms.

CRedit authorship contribution statement

Wenmin Li: Writing – review & editing, original draft, Visualization, Methodology. **Shunsuke Sakai:** Writing – review & editing, Supervision, Methodology. **Zhongkai Zhao:** Writing – review & editing, Supervision, Methodology. **Tatsuhito Hasegawa:** Writing – review & editing, Supervision, Methodology, Resources, Funding acquisition.

Acknowledgements

This work was supported in part by the Japan Society for the Promotion of Science (JSPS) KAKENHI Grant-in-Aid for Scientific Research A (25H01110), B (26K02879), C (23K11164), and the Grant by Marine Informatics Research Institute.

Data availability

The datasets used in this study are publicly available benchmark datasets, including ImageWoof, ImageNette, ImageIDC, CIFAR-10, CIFAR-100, and Tiny-ImageNet. The implementation code and generated distilled samples are

available from the corresponding author upon reasonable request.

Declaration of generative AI and AI-assisted technologies in the writing process

During the preparation of this work, the authors used generative AI tools to assist with language polishing, grammar checking, formatting, and improving the clarity of the manuscript and submission materials. After using these tools, the authors reviewed and edited the content as needed and take full responsibility for the content of the manuscript. No generative AI tool was used to generate research data, perform experiments, conduct analyses, or draw scientific conclusions.

References

- [1] Cazenavette, G., Wang, T., Torralba, A., Efros, A.A., Zhu, J.Y., 2022. Dataset distillation by matching training trajectories, in: Proceedings of the IEEE/CVF Conference on Computer Vision and Pattern Recognition.
- [2] Cazenavette, G., Wang, T., Torralba, A., Efros, A.A., Zhu, J.Y., 2023. Generalizing dataset distillation via deep generative prior. CVPR .
- [3] Chen, M., Du, J., Huang, B., Wang, Y., Zhang, X., Wang, W., 2025. Influence-guided diffusion for dataset distillation, in: The Thirteenth International Conference on Learning Representations. URL: <https://openreview.net/forum?id=0whx8MhysK>.
- [4] Cui, J., Wang, R., Si, S., Hsieh, C.J., 2023. Scaling up dataset distillation to imagenet-1k with constant memory, in: International Conference on Machine Learning (ICML).
- [5] Deng, J., Dong, W., Socher, R., Li, L.J., Li, K., Fei-Fei, L., 2009. Imagenet: A large-scale hierarchical image database, in: Proceedings of the IEEE Conference on Computer Vision and Pattern Recognition (CVPR), pp. 248–255.
- [6] Du, J., Jiang, Y., Tan, V.Y., Zhou, J.T., Li, H., 2023. Minimizing the accumulated trajectory error to improve dataset distillation, in: Proceedings of the IEEE/CVF Conference on Computer Vision and Pattern Recognition (CVPR), pp. 3749–3758.
- [7] Gidaris, S., Komodakis, N., 2018. Dynamic few-shot visual learning without forgetting, in: Proceedings of the IEEE Conference on Computer Vision and Pattern Recognition (CVPR), pp. 4367–4375.
- [8] Goodfellow, I.J., Pouget-Abadie, J., Mirza, M., Xu, B., Warde-Farley, D., Ozair, S., Courville, A., Bengio, Y., 2014. Generative Adversarial Networks URL: <https://arxiv.org/abs/1406.2661>.
- [9] Gu, J., Vahidian, S., Kungurtsev, V., Wang, H., Jiang, W., You, Y., Chen, Y., 2024. Efficient dataset distillation via minimax diffusion, in: Proceedings of the IEEE/CVF Conference on Computer Vision and Pattern Recognition (CVPR), pp. 15793–15803.
- [10] Guo, C., Pleiss, G., Sun, Y., Weinberger, K.Q., 2017. On calibration of modern neural networks, in: Precup, D., Teh, Y.W. (Eds.), Proceedings of the 34th International Conference on Machine Learning, PMLR. pp. 1321–1330. URL: <https://proceedings.mlr.press/v70/guo17a.html>.
- [11] Guo, Z., Wang, K., Cazenavette, G., Li, H., Zhang, K., You, Y., 2024. Towards lossless dataset distillation via difficulty-aligned trajectory matching, in: International Conference on Learning Representations (ICLR).
- [12] He, K., Zhang, X., Ren, S., Sun, J., 2016. Deep residual learning for image recognition, in: Proceedings of the IEEE Conference on Computer Vision and Pattern Recognition (CVPR), pp. 770–778.
- [13] Hendrycks, D., Gimpel, K., 2017. A baseline for detecting misclassified and out-of-distribution examples in neural networks. Proceedings of the International Conference on Learning Representations (ICLR).
- [14] Hinton, G.E., Vinyals, O., Dean, J., 2015. Distilling the knowledge in a neural network. CoRR abs/1503.02531. URL: <http://dblp.uni-trier.de/db/journals/corr/corr1503.html#HintonV15>.
- [15] Ho, J., Jain, A., Abbeel, P., 2020. Denoising diffusion probabilistic models, in: Advances in Neural Information Processing Systems (NeurIPS), pp. 6840–6851.
- [16] Ho, J., Salimans, T., 2022. Classifier-free diffusion guidance. arXiv preprint arXiv:2207.12598 .
- [17] Howard, J., 2019. Imagenette: A smaller subset of 10 easily classified classes from imagenet. <https://github.com/fastai/imagenette>.
- [18] Karras, T., Aittala, M., Aila, T., Laine, S., 2022. Elucidating the design space of diffusion-based generative models, in: Advances in Neural Information Processing Systems (NeurIPS).
- [19] Kim, J.H., Kim, J., Oh, S.J., Yun, S., Song, H., Jeong, J., Ha, J.W., Song, H.O., 2022. Dataset condensation via efficient synthetic-data parameterization, in: Proceedings of the 39th International Conference on Machine Learning (ICML), pp. 11102–11118.
- [20] Krizhevsky, A., Hinton, G., et al., 2009. Learning multiple layers of features from tiny images .
- [21] Le, Y., Yang, X., 2015. Tiny imagenet visual recognition challenge. CS 231N 7, 3.
- [22] Liu, Z., Mao, H., Wu, C.Y., Feichtenhofer, C., Darrell, T., Xie, S., 2022. A convnet for the 2020s, in: Proceedings of the IEEE/CVF Conference on Computer Vision and Pattern Recognition (CVPR), pp. 11976–11986.
- [23] Loo, N., Hasani, R., Lechner, M., Rus, D., 2022. Efficient dataset distillation using random feature approximation, in: Advances in Neural Information Processing Systems (NeurIPS).
- [24] Moser, B.B., Raue, F., Palacio, S., Frolov, S., Dengel, A., 2025. Unlocking dataset distillation with diffusion models. URL: <https://arxiv.org/abs/2403.03881>, arXiv:2403.03881.
- [25] Nguyen, T.C., Chen, Z., Lee, J., 2021. Dataset meta-learning from kernel ridge-regression, in: ICLR 2021. URL: <https://openreview.net/forum?id=l-PrrQrK0QR>.
- [26] Peebles, W., Xie, S., 2023. Scalable diffusion models with transformers, in: Proceedings of the IEEE/CVF International Conference on Computer Vision (ICCV), pp. 4195–4205.
- [27] Qin, T., Deng, Z., Alvarez-Melis, D., 2024. A label is worth a thousand images in dataset distillation, in: The Thirty-eighth Annual Conference on Neural Information Processing Systems. URL: <https://openreview.net/forum?id=oNMnR0NJ2e>.
- [28] Rombach, R., Blattmann, A., Lorenz, D., Esser, P., Ommer, B., 2022. High-resolution image synthesis with latent diffusion models, in: Proceedings of the IEEE/CVF Conference on Computer Vision and Pattern Recognition (CVPR), pp. 10684–10695.
- [29] Sajedi, A., Khaki, S., Amjadi, E., Liu, L.Z., Lawryshyn, Y.A., Plataniotis, K.N., 2023. Datadam: Efficient dataset distillation with attention matching, in: Proceedings of the IEEE/CVF International Conference on Computer Vision (ICCV), pp. 17097–17107.
- [30] Santiago, J.A.C., praveen tirupattur, Nayak, G.K., Liu, G., Shah, M., 2025. MGD³: Mode-guided dataset distillation using diffusion models. URL: <https://openreview.net/forum?id=vKJ8YH0iNp>.
- [31] Sener, O., Savarese, S., 2018. Active learning for convolutional neural networks: A core-set approach, in: International Conference on Learning Representations (ICLR).
- [32] Settles, B., 2009. Active Learning Literature Survey. Technical Report 1648. University of Wisconsin-Madison.
- [33] Shang, Y., Yuan, Z., Yan, Y., 2023. Mim4dd: Mutual information maximization for dataset distillation, in: Advances in Neural Information Processing Systems (NeurIPS).
- [34] Song, J., Meng, C., Ermon, S., 2021. Denoising diffusion implicit models, in: International Conference on Learning Representations (ICLR).
- [35] Su, D., Hou, J., Gao, W., Tian, Y., Tang, B., 2024. D4m: Dataset distillation via disentangled diffusion model, in: CVPR, pp. 5809–5818. URL: <https://doi.org/10.1109/CVPR52733.2024.00555>.
- [36] Sun, P., Shi, B., Yu, D., Lin, T., 2024. On the diversity and realism of distilled dataset: An efficient dataset distillation paradigm, in:

- Proceedings of the IEEE/CVF Conference on Computer Vision and Pattern Recognition (CVPR), pp. 9390–9399.
- [37] Wang, H., Zhao, Z., Wu, J., Shang, Y., Liu, G., Yan, Y., 2025. Cao₂: Rectifying inconsistencies in diffusion-based dataset distillation. URL: <https://arxiv.org/abs/2506.22637>, arXiv:2506.22637.
 - [38] Wang, K., Zhao, B., Peng, X., Zhu, Z., Yang, S., Wang, S., Huang, G., Bilen, H., Wang, X., You, Y., 2022. Cafe: Learning to condense dataset by aligning features, in: Proceedings of the IEEE/CVF Conference on Computer Vision and Pattern Recognition (CVPR), pp. 12196–12205.
 - [39] Wang, T., Zhu, J.Y., Torralba, A., Efros, A.A., 2020. Dataset distillation. URL: <https://arxiv.org/abs/1811.10959>, arXiv:1811.10959.
 - [40] Ye, L., Hamidi, S.M., Li, G., Ogawa, T., Haseyama, M., Plataniotis, K.N., 2025. Information-guided diffusion sampling for dataset distillation. URL: <https://arxiv.org/abs/2507.04619>, arXiv:2507.04619.
 - [41] Zhao, B., Bilen, H., 2021. Dataset condensation with differentiable siamese augmentation, in: International Conference on Machine Learning (ICML), pp. 12674–12685.
 - [42] Zhao, B., Bilen, H., 2022. Synthesizing informative training samples with GAN, in: NeurIPS 2022 Workshop on Synthetic Data for Empowering ML Research. URL: <https://openreview.net/forum?id=frAv0jtUMfS>.
 - [43] Zhao, B., Bilen, H., 2023. Dataset condensation with distribution matching, in: Proceedings of the IEEE/CVF Winter Conference on Applications of Computer Vision 2023 (WACV), Institute of Electrical and Electronics Engineers, United States. pp. 6503–6512. URL: <https://wacv2023.thecvf.com/>, doi:a10.1109/WACV56688.2023.00645.
 - [44] Zhao, B., Mopuri, K.R., Bilen, H., 2020. Dataset condensation with gradient matching. CoRR abs/2006.05929. URL: <https://arxiv.org/abs/2006.05929>, arXiv:2006.05929.
 - [45] Zhong, X., Fang, H., Chen, B., Gu, X., Qiu, M., Qi, S., Xia, S., 2025. Hierarchical features matter: A deep exploration of gan priors for improved dataset distillation, Computer Vision Foundation / IEEE. pp. 30462–30471. doi:10.1109/CVPR52734.2025.02836.
 - [46] Zhou, Y., Nezhadarya, E., Ba, J., 2022. Dataset distillation using neural feature regression, in: Advances in Neural Information Processing Systems (NeurIPS).
 - [47] Zou, L., Chen, G., Chen, Y., Zhang, M., 2025. Enhancing diffusion-based dataset distillation via adversary-guided curriculum sampling. URL: <https://arxiv.org/abs/2508.01264>, arXiv:2508.01264.